Scholar Publishing Group
International Journal of Public Health and Preventive Medicine
https://doi.org/10.38007/IJPHPM.2021.020205
ISSN 2789-8377 Vol. 2, Issue 2: 47-60

Electron Microscopic Observation on Biological Characteristics of Tendon Stem Cells in People with Muscle Collision Injury in Pushing Foul

Hua Li

School of Management, Hainan University, Hainan, China

lihua006@hainanu.edu.cn

Keywords: Biological Characteristics of Tendon Stem Cells, Foul Pushing, Muscle Collision Injury, Multi-Directional Differentiation Potential Detection, Electron Microscope Observation

Abstract: The function of the tendon is to connect bones and muscles, transmit the force generated by muscle contraction to the bones, cause joint activity and body movement, and maintain the stability of the joints. Due to excessive use of body impact in the game, the phenomenon of fouling by teammates, resulting in tendon injury and muscle injury, is a common type of sports injury in sports training and daily life, often causing pain and affecting the body's normal ability to coordinate sports. Or even lead to changes in joint load patterns. Therefore, this article studies the biological characteristics of tendon stem cells in people who have been injured by muscle collision in the foul play. In this study, 30 cases of normal tendon stem cells and 10 cases of tendon stem cells from injured muscles were prepared for cell printing. All specimens were not treated with any anti-tumor treatment before surgery. Fix the sample with 3% formaldehyde solution, rinse with distilled water repeatedly, and dry in a clean space. The samples were dried and placed on the AFM stage, using IX-71 inverted phase contrast microscope to observe the dispersion of cells, select cells for scanning. Select the Tapping mode, adjust the laser to coincide with the tip of the needle, and place the laser spot of the detector on the center dot. Perform automatic frequency modulation in the operating software and adjust the probe until the needle tip touches the sample to start scanning. The experimental data shows that the average size of normal tendon stem cells is 221.11nm*173.88nm, and the average size of tendon stem cells of muscle collision injury is 223.75nm*267.73nm. The experimental results showed that the normal tendon stem cells were fresh under the microscope, and the tendon cells were evenly arranged; while the collagen fibers of the tendon stem cells of the injured muscles were partially lysed, and the tendon cells were disorderly arranged.

1. Introduction

1.1 Background and Significance

The development of sports and the enhancement of competitive levels have put forward higher requirements for athletes' training, which is accompanied by an increased risk of sports injuries. In the past 30 years, the incidence of Achilles tendon rupture among athletes has increased dramatically, and about 30% of athletes have terminated their sports careers after Achilles tendon rupture. In recent years, stem cell treatment methods have been successfully applied in clinics and achieved good therapeutic effects. Adipose-derived mesenchymal stem cells (ADSCs) have become a research hotspot in regenerative medicine and tissue engineering due to their easy availability, rapid proliferation in vitro, and low immunogenicity, and have broad therapeutic potential.

After observation and analysis through a microscope, changes in tendon cells can cause changes in extracellular matrix. Changes in extracellular matrix may also lead to changes in tendon cell morphology and function, affecting proliferation, migration, differentiation and apoptosis of tendon cells. Tendon stem cells can be directly transformed into tendon cells after subculture. They have the potential to self-replicate adult stem cells and induce adipogenesis, chondrogenesis, and osteogenic differentiation. They are precursor cells of tendon cells and directly participate in the repair of acute and chronic injury of tendons the key utility cell in the repair of acute and chronic injury of tendon. This study can provide relevant theoretical basis for the clinical application of allogeneic tendon transplantation to repair tendon defects [1-2].

1.2 Related Work

At present, due to the prevalence of sports, many scholars have also researched tendon stem cells in depth. Yang believes that the lack of suitable cell source candidates for cell transplantation has hindered efforts to treat tendon injuries, such as tendon rupture, tendinitis, and tendinopathy. Tendon-derived stem cells (TDSCs) are a class of stem cells that can be used to treat tendon injuries. He isolated TDSCs from 5-month-old Luxi yellow cattle fetal cattle for in vitro culture, and analyzed their biological characteristics using immunofluorescence and reverse transcription polymerase chain reaction (RT-PCR) methods [3]. However, his research argument is not sufficient, and it is not highly relevant to the experimental research of other scholars. Hao study found that tendon-bone healing after anterior cruciate ligament reconstruction is a complex process that seriously affects the patient's prognosis [4]. Govoni study found that the high tension transmitted by tendons and ligaments makes it easy to tear or completely break. The current standard repair technique is the surgical implantation of autologous or allogeneic bone, which will fail with high probability. He currently uses different types and different biomaterials to design tissue engineering alternatives. Mechanical stimulation driven by special equipment can pre-process these structures to a large extent, simulating the local environment in the body. A large number of dynamic culture instruments have been developed and many attractive results have been achieved. Among the tendons that have been used, the tendon stem is the most promising one for reliable stretch-induced tendonogenesis, but the reduced availability of the tendon stem represents a serious limitation to expanding production. Biomaterials used in the manufacture of scaffolds include biomolecules and synthetic polymers, the latter being improved by nanotechnology that reproduces the structure of natural tendons [5].

1.3 Innovation in this Article

The main innovative work of this paper includes the following aspects: (1) This experiment uses

AFM to observe the ultrastructure of aortic endothelial cell surface with high resolution, reaching nanometer level, which can clearly observe the high fat diet. The ultra-structural changes and dynamic evolution of cell membrane surface. (2) Combining the test of muscle condition analyzer and vibration training to evaluate the effect of vibration training, and to show the objective facts of vibration training as the internal performance of muscles, so that training and monitoring can be organically combined.

2. Biological Characteristics of Tendon Stem Cells

2.1 Tendon Structure

Muscles and tendons are an important part of the exercise system. Tendons are dense collagen connective tissue fiber bundles that connect the skeletal muscle belly and bones. They have strong resistance to pressure, tension and friction, but they do not have the ability to contract. It can transmit the strength of skeletal muscle contraction and relaxation across joints, maintain joint stability and cause body movement [6-7]. Heavy load of mechanical force frequently acting on tendons can easily cause tendon damage. Understanding the basic anatomical structure and mechanical properties of tendons is helpful to further explore the causes of tendon damage [8-9]. Tendon is an important component of the skeletal muscle system. It is mainly composed of collagen fibers, proteoglycans, elastane and other substrates and a small number of cells. Among them, collagen fibers are the most important components of tendons. Their main role is to withstand and conduct different sizes. Tensile load and react to it [10-11]. Among adult tendons, 95% is type I collagen, which plays a role in stabilizing tissue. IHI type collagen, type IV collagen and collagen fibrils with smaller diameters account for about 5% of the total, mainly in immature tendons And in damaged tendon tissue, and different types of collagen fibers have different functions in tendon tissue [12]. Fibroblasts and tendon cells can synthesize and secrete extracellular matrix such as collagen and maintain the metabolism of tendon tissue, which is the basic functional unit of tendon. Tendon cells have a high degree of differentiation. After multiple passages in vitro, the phenotype of tendon cells will change, and the secretion of collagen and proteoglycan will be reduced, which will affect the function of tendon.

2.2 Detection of Stem Cell Multi-Directional Differentiation Potential

(1) Osteogenic differentiation and detection

Take P3 generation cells, after the cells are cultured to 90% confluence, inoculate the cells in a 12-well plate, and inoculate 20,000 cells/well. After the cells adhere to the wall, add osteoblast induction condition medium and change the medium every 3 days. After induction culture for 3 weeks, the culture medium was sucked off and washed 3 times with PBS; 4% paraformaldehyde was fixed at room temperature for 20 min; deionized water was washed to remove paraformaldehyde; then Alizarin red S staining solution was added and stained at room temperature for 5 to 10 min; Clean PBS, observe with microscope and take pictures.

(2) Adipogenic differentiation and detection

The P3 generation cells were taken and cultured to nearly 80% confluence, and adipocyte induction solution was added, and the medium was changed every 3 days. After induction culture for 3 weeks, the medium was sucked off and washed three times with PBS; 4% paraformaldehyde was fixed at room temperature for 20 minutes; deionized water was washed to remove paraformaldehyde; each well was added an appropriate amount of 60% isopropanol solution, mixed

well, and kept static Set for 5 min; absorb isopropanol, add Oilred 0 staining working solution, stain for 5 min; wash 3 times with PBS, observe with microscope and take pictures.

(3) Differentiation and detection of chondrogenesis

Take 1*106 tendon-derived cells from the P3 generation, centrifuge at 300g for 5 minutes until all the cells sink to the bottom of the centrifuge tube, add chondrocyte induction solution at 37 degrees, and culture at 5% CO2. Change the medium every 3 days and induce culture for 3 weeks Around 4% paraformaldehyde is fixed at room temperature for 4 hours. OCT is embedded and frozen for sectioning. After washing the sections with PBS, they were stained with Alcian blue. After the staining, xylene was transparent. After neutral resin was mounted, the microscope was observed and photographed.

2.3 Selection of Cell Labeling Methods

To detect the survival and function of cells transplanted into the body, cell tracers are needed. Currently, commonly used cell labeling methods include fluorescent labeling, radioisotope labeling, and green fluorescent protein gene labeling.

Fluorescent markers are inserted into the biomass membrane and make lateral diffusion movement in the membrane, thereby marking the entire cell. Hepatocytes, fibroblasts, skeletal muscle cells, etc. have been successfully labeled. However, due to the problem of fluorescence attenuation, the tracking time of the mark is limited. In addition, when ultra-thin specimens are sliced, the stain will diffuse into the tissue gap. Although cryopreservation can delay the diffusion process, the problem of background "contamination" caused by diffusion cannot be fundamentally solved.

Radioisotope labeling is a technical method that uses photosensitive materials to analyze the distribution position and content of radioisotope labeled materials in test samples. Isotopic markers can achieve cell tracking by specifically labeling the nucleus. The isotope H has a half-life of up to 12 years and can achieve continuous labeling, so it is the most widely used. The disadvantage of this labeling method is that it will cause experimental artifacts. The reason is that the markers that cannot survive or damage the cells will be engulfed by the body's macrophages along with cell debris, and will be transferred to the lymphatic circulation system for at least 5 Months. Secondly, the isotope incorporated into DNA for cell labeling will also be affected by many factors. For example, the isotope will generate impurities due to the self-decomposition of radiation during storage, and the nucleotide phosphorylase in the cytoplasm can degrade H. Furthermore, the incorporation rate is also related to the type of culture medium, culture time, culture temperature, animal type, age, etc. In addition, because the cells injected into the body cannot continue to obtain isotopes from the surrounding materials, unlike conventional in vivo tracking-radioactive autoradiography, the radioactive intensity of such labeled autoradiography is significantly weaker, which is not conducive to observation.

In this study, Green Fluorescent Protein (GFP) was used as a tracer. Since GFP has been used as a marker for gene expression, GFP has been widely used in the field of molecular biology as a new type of reporter molecule. Its molecular weight is 29KD, the fluorescence emission peak is at 488nm, and the maximum excitation wavelength is 509m. It can be continuously produced in the cell without affecting the cell's own metabolism and protein synthesis. It will emit green fluorescence after absorbing ultraviolet light and blue light, and its fluorescence is extremely Stable, photobleaching resistance is stronger than fluorescein, no germline dependence, and can be expressed in a variety of heterologous cells, so GFP is very suitable as a reporter molecule for

detecting the expression of target genes in cells, locating and quantifying the expression of foreign genes analysis.

2.4 Imaging Theory of Confocal Microscopy System

Reflective infinity confocal microscopy system includes microscope objective lens, illumination lens, focusing lens, beam splitter, light source, pinhole and detector. The lens can be regarded as a phase object, and the phase and amplitude of the wave field of the light wave entering the lens changes. If only the phase transformation of the ideal thin lens is considered, the complex amplitude form of the thin lens transmittance is:

$$t(x,y)=\exp\left[-j\frac{k}{2f}\left(x^2+y^2\right)\right] \tag{1}$$

In the formula, f is the focal length of the thin lens, $k=\frac{2\pi}{\lambda}$ is the wave number of incident light, and λ is the light wavelength. Therefore, under the paraxial approximation, the transmission function of the thin lens is:

$$T(x,y)=P(x,y)\exp\left[-j\frac{k}{2f}\left(x^2+y^2\right)\right] \tag{2}$$

Among them, P (x, y) is the pupil function of the thin lens, which characterizes the range limit of the incident wavefront of the lens, which can be expressed as:

$$P(x,y)=\begin{cases}1 & \text{Within the aperture}\\ 0 & \text{Other}\end{cases} \tag{3}$$

If the complex amplitude of the incident light wave of the system is A0, the complex amplitude of the incident light wave in front of the microscope objective L2 is affected by the pupil function P1 of the illumination lens LI and becomes:

$$U_{-1}(x_1,y_1)=A_0P_1(x_1,y_1) \tag{4}$$

The lens phase-modulates the incident light wave, so the light field is modulated by the microscope objective L2, and the complex amplitude becomes:

$$U_{+1}(x_1,y_1)=U_{-1}(x_1,y_1)T_2(x,y) \tag{5}$$

In the formula, T2(x, y) is the transmittance function of the microscope objective L2. Since Px(x, y) is the pupil function of the microscope objective L2, the transmission function of the microscope objective L2 is:

$$T_2(x,y)=P_2(x_1,y_1)\exp\left[-j\frac{k}{2f_2}\left(x_1^2+y_1^2\right)\right] \tag{6}$$

$$U_{+1}(x_1+y_1)=A_0 P_1(x_1,y_1)P_2(x_1,y_1)\exp\left[-j\frac{k}{2f_2}\left(x_1^2+y_1^2\right)\right] \tag{7}$$

According to equation (7), the complex amplitude U+(x,y) of the incident light wave after passing through the microscope objective L2 is affected by the pupil function Pr(x, y) of the illumination lens LI and the pupil function P2 of the microscope objective L2 (x, y) work together; according to equation (3), the pupil function is related to the lens aperture.

3. Observation Experiment of Tendon Stem Cells in Muscle Collision Injury

3.1 Experimental Objects and Instruments

Subjects: 60 Sprague Dawley (SD) rats, with an average of about two hundred grams, male, purchased from an animal experiment center. All animal feeding and experiments in this study were in compliance with relevant animal welfare and medical ethics regulations. The experimenters all passed the relevant animal experiment assessment, and the experiment site is located in the animal experiment center. Experimental instruments include HF100 37.5C 5% CO2 incubator, DL-CJ-2N high-performance aseptic test bench, TDZS-WS multi-tube rack automatic balancing centrifuge, 1-15K high-speed centrifuge, electronic analytical balance BS 124S, IX- 71 inverted phase contrast microscope, CX31 biological microscope, TE-2000-E laser scanning confocal microscope, stereo microscope OLYMPUS SZ61, HH-4 digital display constant temperature water bath, YYQ-LS-70A automatic electric pressure steam sterilizer, PH033A Type incubator/dryer, 84-1A magnetic stirrer, Pall ultrapure water meter, BCD-539 ultra-low temperature refrigerator, disposable plastic culture m, blood cell counting plate, liquid nitrogen reservoir, ND-1000 spectrophotometer, PCR Amplifier. The TE-2000-E laser scanning confocal microscope used in the experiment is shown in Figure 1(figure come from www. baidu. com).

Figure 1: TE-2000-E laser scanning confocal microscope

3.2 Main Experimental Steps

The experiment was divided into two groups, a normal group and a muscle injury group. SD rats in the normal group were intraperitoneally injected with 0.2ml/100g of physiological saline, and SD rats after muscle injury were intraperitoneally injected with pentobarbital sodium 0.2ml/100g, cut off in the neck, and immersed in 75% alcohol 5- After 10 minutes, the transitional part of the tendon bone and the junction of the tendon and muscle of the patellar tendon tissue of the rat were removed under sterile conditions. Carefully remove the aponeurosis on the surface of the tendon, immerse the sample in sterile PBS, cut the tendon tissue into small pieces of lmm*lmm*lmm, put them in a Petri dish, and digest with 0.3% type I collagenase (3mg/ml) 2.5h, and gently pipette with a 3ml pipette, filter the digested cell and tissue suspension with a 70μm cell filter (BD Biosciences) and collect single cell suspension. The cells were washed with PBS and centrifuged at 300g for 5 min to remove the supernatant, and the cells were resuspended with basal medium (LG-DMEM, volume fraction 10% fetal bovine serum, 1% double antibody). The cell suspension was inoculated into a 20 cm2 petri dish at a cell density of 50 cells/cm^2, and the medium was changed for the first time on the second day, and washed twice with PBS to remove cells that did not adhere. After culturing for about 7 days, cells were digested with 0.25% trypsin (EDTA) and mixed, and labeled as primary cells. After the cells were covered with 90% of the bottom of the culture flask, the cells were passaged. The culture solution was discarded, washed twice with PBS, digested with 0.25% trypsin (EDTA) for 2-3 min, and basal medium was added to terminate the digestion. The suspension was centrifuged at 1000 rpm for 5 min. Discard the supernatant, add 2ml of basal medium to resuspend the cells and count, and inoculate the flask at a density of 5*103/cm2. The third generation of tendon thousand cells (TDSCs) was used for subsequent experiments. Observe the cell growth under an inverted microscope.

3.3 Data Collection

SPSS 20.0 software (SPSS, Chicago, IL) was used for data analysis and processing. The comparative analysis of the biological characteristics of tendon stem cells and each test index of the control group used independent sample t test. The measurement data of the research data are recorded in the form of mean±standard deviation, and the statistical value of all parameters is statistically significant with $P<0.05$.

4. Data Analysis of Biological Characteristics of Tendon Stem Cells

4.1 Observe the Changes of Cell Membrane of Each Specimen after Heating under Afm

As far as this experiment is concerned, after heating, the specimens are all surviving cells and dead cells. When analyzing the image results, we will organize all the pictures of each specimen, divide the structural changes into similar groups, and combine the specimens. Cell death rate, to determine which group of images is the surface structure of the surviving cell membrane, which group is the surface structure of the dead cell membrane. When the scanning range is 500nm, the study found that after the cells are heated, the above three cell membrane surface structures have similar changes and also have their own unique performance. The specific data is shown in Table 1, and the specific image is shown in Figure 2.

Table 1: Comparison of the membrane structure of Fb cells and Hela cells in each time period heated at 41 degrees (nm)

	FB cell		Hela cell	
	Bulge size	Height on Z axis	Bulge size	Height on Z axis
37 degrees Celsius	81.24*55.10	49.36	71.74*32.15	32.63
41 degrees Celsius 30min	89.36*63.52	36.25	78.36*45.36	24.36
41 degrees Celsius 1h	121.54*72.41	59.63	96.14*57.96	42.51
41 degrees Celsius 2h	128.36*75.14	43.25	95.32*59.25	35.56

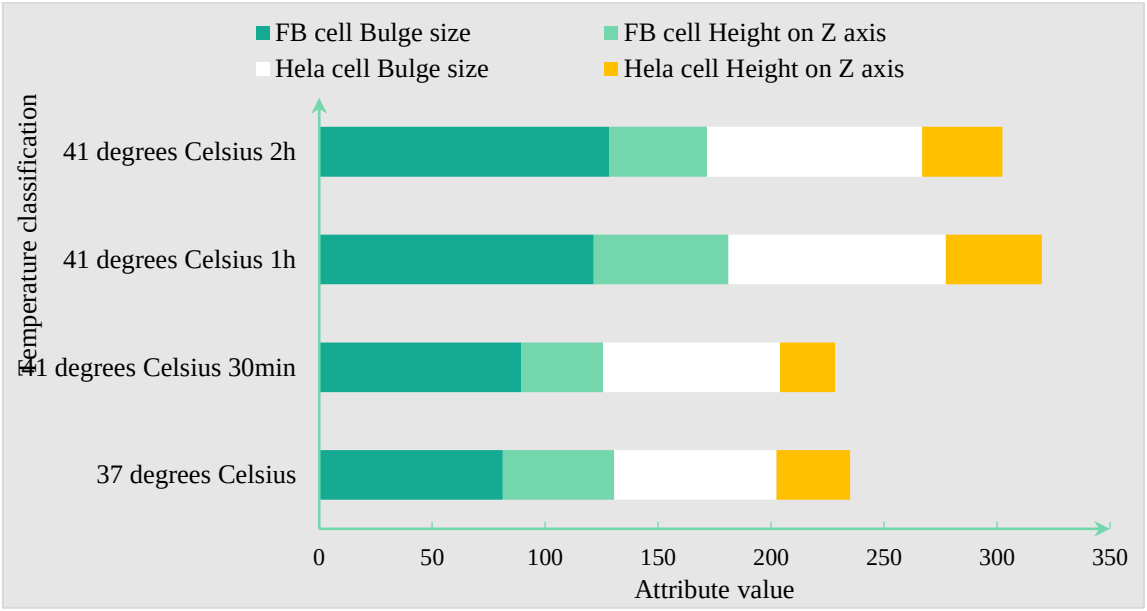

Figure 2: Comparison of membrane structure between Fb cells and Hela cells heated at 41 degrees

Similarities: The cell membranes of all specimens show a fusion trend. The same heating time and different temperatures have different effects on the cell membrane, but there are certain regularities. With the increase of temperature, the process of bulging structure change on the surface of the cell membrane is as follows: the boundary between the cells will be clearer, the blurry boundary will fuse into pieces, the shape will be fuller, and the surface will be uneven after fusion. During this change, the height of the uplift is gradually increasing.

Differences: At 41 ℃, only some areas of the bulge structure on the cell membrane of the specimen are fused, while the original structures such as bulge and depression of the cell membrane in other areas still exist, but the bulge structure generally increases, and the height change in the Z axis direction is not obvious Regularity (this may be related to the limited number of cells scanned at present, which may lead to deviations in statistical accuracy). The uplift structure on the surface of the cell membrane of the specimen at 43 degrees and 30 minutes merged into a number of larger protrusion structures, and the depression was obviously widened. The original structure in some areas was still vaguely visible, and the height of the uplift structure in the Z axis direction was significantly increased. The cell membranes of the specimens at other times of 43 degrees and the specimens of each time of 48 degrees almost completely lost the original structure, and replaced with larger bulges and widened concave structures after fusion. The height of each ridge on the Z axis is still increasing, 5- a: When the scanning range is 500nm, the cell membrane structure of each

specimen of Hela cells at 41 degrees 30min, 43 degrees 30min, 48 degrees 30min; 5-b: When the scanning range is 500nm, Hela cells 41 degrees 1h, 43 degrees 1h, 48 degrees 1h Membrane structure of specimens; 5-c: When the scanning range is 500 nm, the membrane structure of specimens of Hela cells at 41 degrees 2h, 43 degrees 2h, 48 degrees 2h.

In addition, we also found that the Fb cell membrane appeared a spherical structure at 43 degrees 1h. The spherical structure protruded out of the cell and seemed to separate from the cell membrane. The average size was 221.11nm*173.88nm, 43 degrees 1h Hela cell specimens and 48 The structure was also found in specimens of Mcf7 cells at 30 min. The average size was 223.75nm*267.73nm151.96nm*190.02nm. In the same book, the volume of the ball structure is not much different, and the number is indefinite.

4.2 Cell Viability of Tscs after Spio Labeling

TSCs with high expression of NS, SSEA4 and OCT4 were used for labeling. The experiment found that TSCs ingested SPIO through endocytosis, which showed that SPIO was in the cytoplasm and surrounded the nucleus. The cell labeling rate is about 98%. The cell morphology of TSCs labeled with SPIO was not significantly changed, and the cell proliferation was not significantly changed. It was shown that there was no significant statistical difference between PDT and unlabeled TSCs (P>0.05). The specific data is shown in Table 2 and the image is as follows Figure 3 shows that SPIO labeling does not affect the proliferation function of cells. The cell viability was detected at 2, 4, and 7 days after labeling, and it was found that the viability was about 90%, and there was no significant difference compared with unlabeled cells, indicating that SPIO labeling does not significantly interfere with the cell viability of TSCs (P>0.05) The specific data is shown in Table 3, and the specific image is shown in Figure 4.

Table 2: Effect of SPIO marking on PDT of TSCs

	Mean ±SD			F value	P value
	Control	P-PRP	L-PRP		
Adipo	36.888 ±5.216	32.331 ±5.261	86.215 ±5.326	112.415	0
Chondro	62.888 ±3.251	78.215 ±4.265	82.360 ±3.965	62.351	0
Osteo	42.888 ±6.352	45.362 ±3.251	110.314 ±4.215	49.364	0

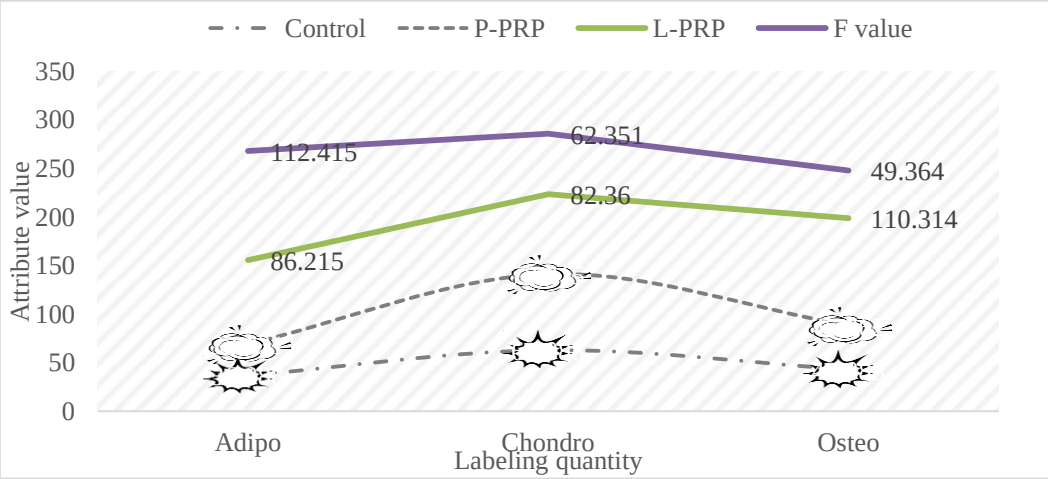

Figure 3: Effect of SPIO marking on PDT of TSCs

Table 3: Cell viability of SPIO markers on TSCs

	Labeled	Non-labeled	T value	P value
Day2	0.925±0.055	0.921±0.407	0.3625	0.785
Day4	0.936±0.036	0.814±0.564	1.5632	0.362
Day7	0.985±0.014	0.783±0.325	-2.385	0.631

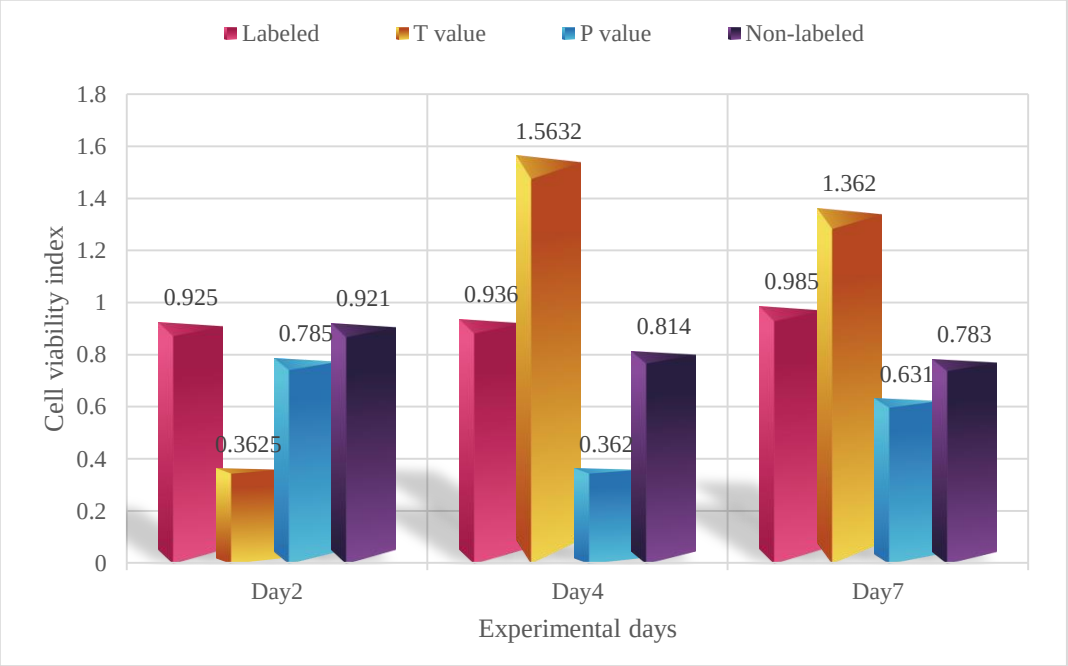

Figure 4: SPIO labeling on cell viability of TSCs

Figure 4 confirms that SPSC labeling of TSCs will not affect its dryness. SPSC-labeled TSCs in vivo and in vivo can be effectively traced by MRI. P-PRP glue is a good carrier of TSCs by MRI dynamic observation and immunohistochemistry. Because SPIO labeling does not significantly affect the proliferation and differentiation of TSCs, TSCs can be evenly distributed in P-PRP gel and the labeled TSCs cell concentration is linearly related to the MRI signal. P-PRP gel TSCs complex repairs the rabbit patellar ligament window type No obvious radiographic changes were observed in MRI observations at 2 and 3 weeks after the defect. The structure of MRI development confirmed by Pluck's blue staining is SPIO-labeled TSCs, indicating that P-PRP glue can stably maintain TSCs at the target site. It was confirmed by immunohistochemistry that TSCs retain their ability to synthesize type I collagen after being implanted in the body for 3 weeks, indicating that P-PRP glue is a good carrier for TSCs.

4.3 Histological Observation of Mouse Tendon

The normal tendon tissue is white to the naked eye, easy to peel off from the muscle when dissecting, and has strong toughness and neat edges; the paraffin tissue section of normal tendon after H&E staining can be seen under the light microscope with fresh color, the tendon cells are arranged evenly, and the collagen fibers are arranged neatly, Dense, smooth tendon tissue edges, the specific image shown in Figure 5. Twenty-four hours after the injection of collagenase type I, the

right limb of the mouse was swollen obviously, and the volume of the tendon was reduced or partly damaged during dissection, and it was adhered to the surrounding tissues, with poor toughness, not easy to peel, and the edges were rough; collagenase after H&E staining In the induced injury group, the collagen fibers of the tendon tissue of the mice were partially lysed, the arrangement of tendon cells was disordered, and the tissue defect was more serious. The specific image is shown in Figure 6.

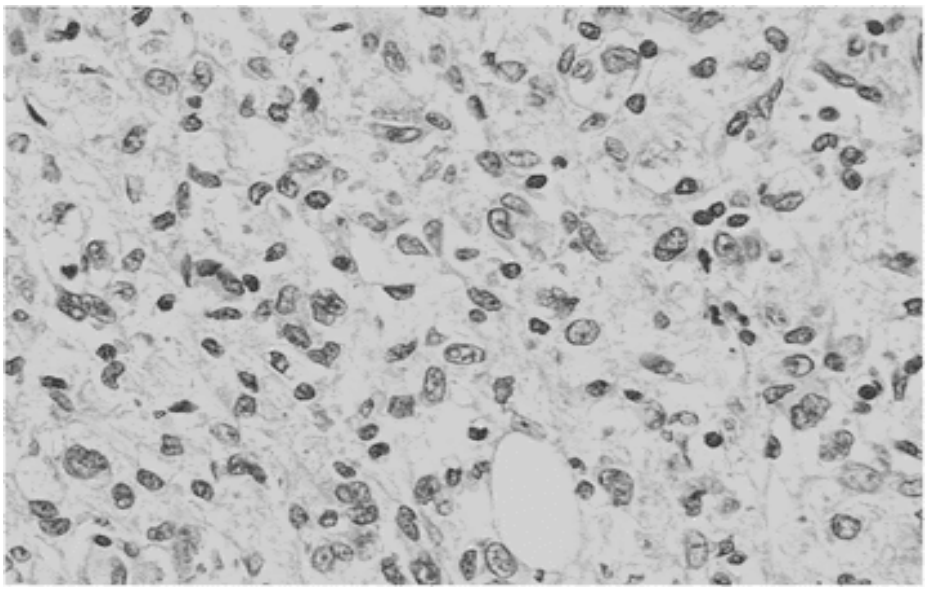

Figure 5: Histological Observation Of Normal Tendon Cells In Mice

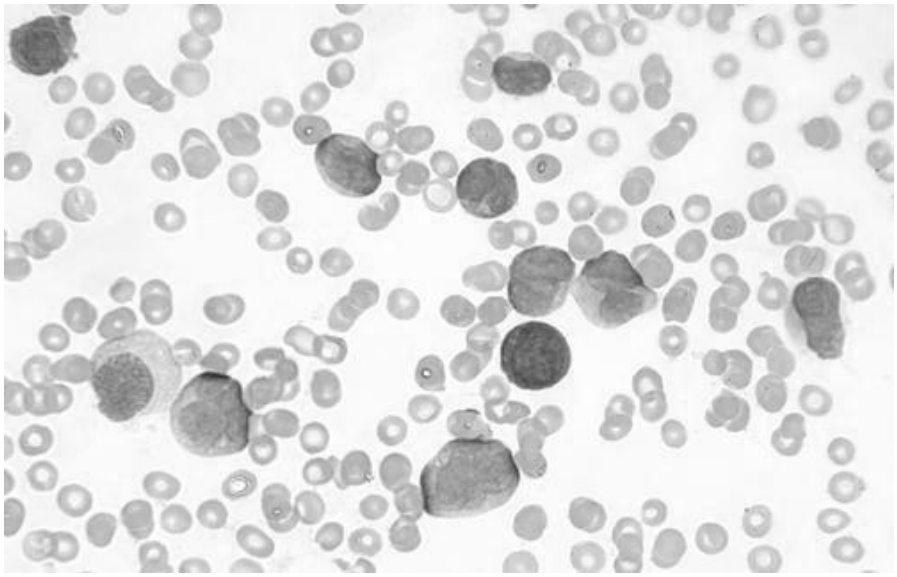

Figure 6: Histological Observation Of Mouse Tendons With Abnormal Tendon Cells

It can be seen from Figure 6 those 24 hours after transplantation of ADSCs, some inflammatory cells can be observed to gather at the damaged site of tendon, and a large number of inflammatory cells accumulate at the tissue injury site from 3d to 5d after transplantation, and microangiogenesis

can be observed. At 21 days after transplantation, the repair of tendon tissue in the ADSCs treatment group was significantly better than that in groups I and IS. The collagen fiber dissolution site was basically filled with cells and extracellular matrix; at 28 days after transplantation, the inflammatory cells in the middle of the tendon tissue were basically evenly distributed, and It spreads around the tendon and the collagen fibers are clearly distinguishable. After transplantation 35, the inflammatory cells on the periphery of the tendon tissues are further reduced, and the collagen fibers are arranged in an orderly and tight manner, which basically returns to the normal group. Tendons in the injured group have the function of self-repair. Tension tissues in group I and group IS have also undergone inflammatory cell aggregation (1-14d) and regression (21d-35d), but the collagenase damage and dissolution are still in a defect state at 35 days. The tendon cells are unevenly distributed and the collagen fibers tend to be chaotic.

4.4 Specific Gene Analysis of Tendon Stem Cells

The identification of TDSCs specifically expressed genes and surface markers was used to identify tendon stem cells in the study. In this study, RT-PCR and immunofluorescence were used to specifically express the tendons such as collagen I, CD44, Nucleostemin and Tenascin-C the gene and surface markers were tested, and the results were all positive. The positive rate of cells was analyzed by the loss-cell technique and the positive rates of collagenI, CD44, and Tenascin-C cells were all above 90%. Experiments show that the tendon is mainly composed of fibroblasts and extracellular matrix, which is dense connective tissue. The extracellular matrix is mainly composed of collagen, forming a dense and parallel arrangement of collagen fiber bundles. A small amount of proteoglycan and Glycosaminoglycans are connected, and different subtypes of collagen play an important role in the formation of tendons.

Tenascin C is a gene specifically expressed by tendon cells, and its expression usually appears in the fibrocartilage of the bone tendon junction. The expression of this gene here indicates that the tendon stem cells may be involved in the generation and reconstruction of fibrocartilage at the bone tendon junction. Not only does it show that TDSCs have the characteristics of stem cells, but also that TDSCs have the characteristics of tendon cells. CD44 is a cell surface glycoprotein, which is classified as an adhesion molecule that mediates cell-cell and cell extracellular matrix interactions, and usually binds to type I collagen and fibronectin. The function of CD44 is controlled by its post-translational modifications and plays an important role in many physiological processes. The protein is also involved in a wide range of cell functions, including activation, recycling and homing of lymphocytes, and as an important marker of the repair phase after various tissue injuries. Nuclear stem cell factor is only expressed in the nucleus of stem cells and some tumor cells, but the terminal cells cannot be expressed. In this study, the gene RT-PCR test results were positive, thus inferring that the TDSCs isolated and cultured in this experiment have the characteristics of stem cells., Also verified the identification results of tendon stem cells.

5. Conclusions

This study successfully established an in vitro separation, culture and expansion system for mouse adipose-derived mesenchymal stem cells. The cultured adipose-derived mesenchymal stem cells have strong self-renewal and proliferative capabilities, and can be passed to 50 generations in vitro. The characteristics of stem cells and low immunogenicity will not be changed by multiple passages. The transplanted adipose-derived mesenchymal stem cells can quickly migrate to the site of type I collagenase-induced tendon injury in mice, expressing tendon cell-related proteins, and

promoting the regeneration and repair of tendon tissue.

Both the normal group and the muscle injury group tendon stem cell tissue contained tendon stem cells with cloning formation ability and multi-directional differentiation potential. The number of tendon stem cells in the muscle injury group was reduced compared with the normal group. Tendon stem cells derived from muscle injury group and normal group derived tendon have similar cell proliferation ability, early apoptosis rate, in vitro migration ability and tendon differentiation ability in vitro. Muscle injury reduces the survival rate of nucleated cells in rat tendon tissue, but tendon tissue still retains a large number of active stem cells. Although the number of tendon stem cells in the experimental group decreased, compared with the control group, there was no obvious abnormality in cell proliferation ability, early apoptosis rate, in vitro migration ability and tendon differentiation ability.

The use of PI staining in this study ruled out the possibility of pits on the cell membrane surface. AFM has been applied to the imaging of proteins, DNA, viruses and other biological samples. However, AFM has not been used to image holes in real cell membranes in previous studies. In this study, the AFM of the taskforce mode was used to vibrate the probe tip in a sinusoidal manner, the results of probing the sample surface at high frequency and recording a series of force curves for each pixel on the sample, by adjusting the vertical piezoelectric driver (z-piezo) come hold on to the maximum peak force. The z-piezoelectric motion of the probe is then plotted as a 3D topology of the sample as a function of x, y horizontal coordinates. The fixed oscillation frequency applied in the peak force mode is much lower than the probe cantilever resonance frequency, which subtly suppresses long-range interaction forces such as adhesion and electrostatic forces, thereby significantly improving image quality and reducing human error. SD mice were used as the research object to trace the peripheral nerve cells. In the designed patellar tendon window injury and Achilles tendon rupture model, the characteristics of RFP-labeled nerve cells surrounding neovascular tissue were found. Immunofluorescence staining of the injury site identified that peripheral nerve cells quickly budded and migrated into the injury site, some nerve tissue secreted nerve peptides, and the neovascularization tissue produced more obvious nerve peptide receptors (Neuropeptide Y1 receptor), indicating that the two The authors show significant relevance.

References

[1] Chen, Y. Y., He, S. T., Yan, F. H., Zhou, P. F., Luo, K., & Zhang, Y. D., et al. (2016). "Dental pulp stem cells express tendon markers under mechanical loading and are a potential cell source for tissue engineering of tendon-like tissue,"International Journal of Oral Ence,8(004),pp. 213-222. https://doi.org/10.1038/ijos.2016.33

[2] López-Nájera, Diego, Rubio-Zaragoza, Mónica, Sopena-Juncosa, Joaquín J., Alentorn-Geli, E., Cugat-Bertomeu, Ramón, & Fernández-Sarmiento, J. Andrés, et al. (2015). "Effects of plasma rich in growth factors (prgf) on biomechanical properties of achilles tendon repair", Knee Surgery Sports Traumatology Arthroscopy, 24(12), pp.1-8.

[3] Yang, J., Zhao, Q., Wang, K., Liu, H., Ma, C., & Huang, H., et al. (2016). "Isolation and biological characterization of tendon-derived stem cells from fetal bovine", In Vitro Cellular & Developmental Biology. Animal, 52(8), pp.846-856. https://doi.org/10.1007/s11626-016-0043-z

[4] Hao, Z. C., Wang, S. Z., Zhang, X. J., & Lu, J. (2016). "Stem cell therapy: a promising biological strategy for tendon–bone healing after anterior cruciate ligament reconstruction",Cell Proliferation,49(2),pp. 154-162. https://doi.org/10.1111/cpr.12242

[5] Govoni, M., Muscari, C., Lovecchio, J., Guarnieri, C., & Giordano, E. (2016). "Mechanical

actuation systems for the phenotype commitment of stem cell-based tendon and ligament tissue substitutes",Stem Cell Reviews & Reports,12(2), pp.189-201. https://doi.org/10.1007/s12015-015-9640-6

[6] Bavin, E. P., Atkinson, F., Barsby, T., & Guest, D. J. (2017). "Scleraxis is essential for tendon differentiation by equine embryonic stem cells and in equine fetal tenocytes", Stem Cells & Development, 26(6), pp. 441-450. https://doi.org/10.1089/scd.2016.0279

[7] Bianco, S. T., Moser, H. L., Galatz, L. M., & Huang, A. H. (2019). "Biologics and stem cell - based therapies for rotator cuff repair. Annals of the New York Academy of Sciences, 1442(APR.), pp. 35-47. https://doi.org/10.1111/nyas.13918

[8] Bohá, Martin, Csbnyeiová, Mária, Kupcová, Ida, Zamborsky, R., Fedele, J., & Koller, Ján. (2016). "Stem cell regenerative potential for plastic and reconstructive surgery", Cell & Tissue Banking, 17(4), pp.1-10. https://doi.org/10.1007/s10561-016-9583-4

[9] Sharma, N. N., Carmai, J., Koetniyom, S., & Markert, B. (2016). "Effects of active muscle contraction on whiplash injury", PAMM, 16(1), pp.105-106. https://doi.org/10.1002/pamm.201610041

[10] Du, X., Zhang, G., Cao, L., & Hu, Y. (2016). "A study on the simulation analysis and injury criterion of chinese lower leg impact", Qiche Gongcheng/Automotive Engineering, 38(11), pp.1324-1330.

[11] Gao, Z., Li, Z., Hu, H., & Gao, F. (2019). "Experimental and numerical study of cervical muscle contraction in frontal impact", Automotive Innovation, 2(2), pp.93-101.

[12] Fice, J. B., Siegmund, G. P., & Blouin Jean-Sébastien. (2018). "Neck muscle biomechanics and neural control", Journal of Neurophysiology, 120(1), pp.361-371. https://doi.org/10.1152/jn.00512.2017